Optica Applicata, Vol. LV, No. 4, 2025
DOI: 10.37190/oa/209625

Performance analysis of hybrid RF/FSO link over Nakagami-*m* fading and Chi-square–inverse Gamma atmospheric turbulence with pointing errors

Majid Hamid ABDULLAH[1], Nenad STANOJEVIĆ[2,*], Stefan PANIĆ[3,*], Petar SPALEVIĆ[2], Đorđe ŠARČEVIĆ[1], Srdjan MITROVIĆ[1]

[1] School of Informatics and Computing, Singidunim University, Danijelova 32, 11000 Belgrade, Serbia

[2] Faculty of Technical Sciences, University of Priština – Kosovska Mitrovica, Knjaza Miloša 7, 38220 Kosovska Mitrovica, Serbia

[3] Faculty of Sciences, University of Priština – Kosovska Mitrovica, Lole Ribara 29, 38220 Kosovska Mitrovica, Serbia

[*]Corresponding authors: nenads25@gmail.com (N.S.), stefan.panic@pr.ac.rs (S.P.)

This paper introduces a novel statistical model for the performance analysis of hybrid RF/FSO (radio frequency/free-space optics) communication systems. The RF channel is modeled using the Nakagami-*m* fading distribution, while the FSO channel is characterized by a Chi-square–inverse Gamma distribution to account for atmospheric turbulence and pointing errors. A closed-form expression for the cumulative distribution function (CDF) of a one-hop hybrid RF/FSO system is derived under a selective combining scheme, formulated as a function of the average signal-to-noise ratio (SNR). The resulting CDF is expressed in terms of the extended generalized bivariate Meijer-*G* function (EGBMGF). Furthermore, new analytical expressions for the average bit error rate (ABER) are obtained for both the hybrid RF/FSO system and its FSO-only counterpart under coherent binary phase-shift keying (CBPSK) modulation. A detailed comparative analysis is performed across varying channel parameters and turbulence conditions. Numerical results, presented graphically, demonstrate the superior robustness of the proposed hybrid scheme under severe turbulence and misalignment effects.

Keywords: hybrid RF/FSO system, Nakagami-*m*, Chi-square–inverse Gamma, one-hop, CBPSK.

1. Introduction

Free-space optical (FSO) communication systems have gained significant attention due to their high bandwidth, low deployment cost, and compatibility with optical fiber networks. However, their performance is highly susceptible to adverse weather conditions and temporary loss of line-of-sight (LOS). Numerous studies [1-3] have demon-

strated that fog has the most detrimental effect on optical signal propagation, while rain introduces negligible attenuation. This is attributed to the particle sizes in fog and mist being comparable to optical wavelengths, leading to considerable scattering. Atmospheric attenuation in FSO links is thus primarily caused by scattering, with absorption playing a secondary role, ultimately limiting the channel bandwidth and degrading transmission quality.

To enhance system reliability under such impairments, hybrid architectures have been proposed [4-6]. These systems combine the strengths of radio frequency (RF) and FSO communication. The RF link operates in millimeter-wave bands and remains largely unaffected by fog, while the FSO link offers high data rates in clear weather. In foggy conditions where FSO performance degrades, the RF link ensures communication continuity. Conversely, RF performance degrades under heavy rain, in which case the FSO link takes over [7-10]. This switching mechanism enhances overall link robustness by leveraging the complementary characteristics of RF and FSO channels.

Two main configurations are used in hybrid RF/FSO systems:

1) Simultaneous transmission, where both links operate concurrently, providing high reliability but at the cost of spectral inefficiency.

2) Handover-based transmission, where transmission dynamically switches between RF and FSO links based on channel quality, offering better resource utilization but increased sensitivity to rapid environmental changes [11].

Diversity combining techniques, originally developed for RF systems, have also been adapted for hybrid RF/FSO links to mitigate fading and improve signal robustness [12, 13]. In particular, handover strategies that activate the RF link when the FSO signal-to-noise ratio (SNR) drops below a predefined threshold have proven effective for maintaining link availability.

A one-hop hybrid RF/FSO system, where data is transmitted directly from source to destination without intermediate relays, requires accurate statistical modeling to assess performance. Due to the variability and complexity of weather-induced channel effects, a universal model is not feasible. Therefore, composite statistical models are employed to separately model the RF and FSO components. Prior work [14] used a Gamma-Gamma model for the FSO link and Nakagami-*m* fading for the RF link, demonstrating improvements in average bit error rate (ABER) and outage probability. Similarly, [15] adopted a Málaga distribution for FSO fading and a generalized α-η-k-μ model for RF, showing improved resilience to turbulence and pointing errors.

In this study, we analyze a hybrid one-hop RF/FSO communication system in which the RF fading is modeled using the Nakagami-*m* distribution, and the FSO turbulence is characterized using the Chi-square–inverse Gamma distribution. We derive the cumulative distribution function (CDF) for the composite system based on the product of the independent CDFs of both channels. Furthermore, we propose a new analytical expression for the ABER using coherent binary phase-shift keying (CBPSK) modulation. The performance of the hybrid model is compared to the standalone FSO system under varying turbulence levels and system parameters, illustrating the advantages of the hybrid approach in mitigating atmospheric impairments and misalignment effects.

2. System and channel model

The hybrid RF/FSO system consists of two links, RF and FSO, which use the same digital modulation scheme. At the transmitter, the signal is sent to both the RF and FSO links, where transmission occurs simultaneously over both links. The Nakagami-*m* distribution is used for modeling RF channel fading. The PDF of the Nakagami-*m* distribution, depending on the SNR, can be represented by the expression [14]

$$f_{\gamma_1}(\gamma_1) = \left(\frac{m}{\mu_1}\right)^m \left(\frac{\gamma_1^{m-1}}{\Gamma(m)}\right) G_{0.1}^{1.0}\left(\begin{matrix} - \\ 0 \end{matrix}\middle| \frac{m\gamma_1}{\mu_1}\right) \tag{1}$$

where the fading statistic factor $m \geq 0.5$ represents the relative strength of the fading coefficient, γ_1 denotes the SNR of the RF system, μ_1 represents the average SNR, and Γ denotes the Gamma function.

$$F_{\gamma_1}(\gamma_1) = \int_0^{\gamma_1} f_{\gamma_1}(\gamma_1)\,\mathrm{d}\gamma_1 \tag{2}$$

By substituting expression (1) into (2) and applying the rule (07.34.21.0084.01) from Ref. [16], the integral is solved, and the resulting expression represents the CDF:

$$F_{\gamma_1}(\gamma_1) = \frac{1}{\Gamma(m)} G_{1.2}^{1.1}\left(\begin{matrix} 1 \\ m, 0 \end{matrix}\middle| \frac{m\gamma_1}{\mu_1}\right) \tag{3}$$

For modeling the turbulence of the FSO link, the Chi-square–inverse Gamma distribution was used. The expression for the PDF when IM/DD is applied under the influence of pointing error, in relation to the SNR, is given by the following expression [17]:

$$f_{\gamma_2}(\gamma_2) = \sum_{p=0}^{\infty} \frac{\xi^2 K^p \Gamma(b+\xi^2+1)\exp(-K)}{2\gamma_2(b+\xi^2)\,\Gamma(p+1)\,p!\,\Gamma(b)\,\Gamma(b+\xi^2)}$$

$$\times\, G_{2.2}^{2.1}\left(\begin{matrix} 1-b,\, 1+\xi^2 \\ \xi^2,\, p+1 \end{matrix}\middle| \frac{(K+1)\xi^2}{(b-1)(\xi^2+1)} \sqrt{\frac{\gamma_2}{\mu_2}}\right) \tag{4}$$

where K denotes the Rician factor, which defines the ratio between the direct component and the components resulting from scattering, γ_2 is the SNR of the FSO system, and ξ represents the laser pointing error, calculated as

$$\xi = \frac{w_{\mathrm{L\_eq}}}{2\sigma_{\mathrm{s}}} \tag{5}$$

where σ_{s} is the standard deviation of the pointing error (jitter) at the receiver, and $w_{\mathrm{L\_eq}}$ is the equivalent radius of the received beam

$$w_{\mathrm{L\_eq}}^2 = w_{\mathrm{L}}^2 \frac{\mathrm{erf}(v)\sqrt{\pi}}{2v} \tag{6}$$

where $v = \sqrt{\pi}\, a / \sqrt{\pi}\, w_{\mathrm{L}}$, $A_0 = [\mathrm{erf}(v)]^2$, with $\mathrm{erf}(\cdot)$ denoting the error function. The distribution parameter b can be calculated using the following expression:

$$b = \frac{1}{\exp(\sigma_{\mathrm{ls}}^2) - 1} + 2 \tag{7}$$

and σ_{ls}^2 can be obtained from the expression:

$$\sigma_{\mathrm{ls}}^2 = \sigma_{\mathrm{ls}}^2(l_0) - \sigma_{\mathrm{ls}}^2(L_0) \tag{8}$$

and represents the log-variance of the irradiance, where $\sigma_{\mathrm{ls}}^2(l_0)$ and $\sigma_{\mathrm{ls}}^2(L_0)$ are the effects of large-scale and small-scale eddy fluctuations, respectively.

$$\sigma_{\mathrm{ls}}^2(l_0) = 0.04\sigma_1^2 \left(\frac{\eta_{\mathrm{Xa}} Q_{\mathrm{ls}}}{\eta_{\mathrm{Xa}} + Q_{\mathrm{ls}}}\right)^{7/6} \left[1 + 1.75\left(\frac{\eta_{\mathrm{Xa}}}{\eta_{\mathrm{Xa}} + Q_{\mathrm{ls}}}\right)^{1/2} - 0.25\left(\frac{\eta_{\mathrm{Xa}}}{\eta_{\mathrm{Xa}} + Q_{\mathrm{ls}}}\right)^{7/12}\right] \tag{9}$$

where:

$$\eta_{\mathrm{Xa}} = \frac{8.56}{1 + 0.18^2 + 0.2\sigma_{\mathrm{R}}^2 Q_{\mathrm{ls}}^{1/6}} \tag{10}$$

$$Q_{\mathrm{ls}} = \frac{10.89 L}{k l_0^2} \tag{11}$$

while k denotes the wave number, λ is the wavelength, l_0 represents small-scale eddies (expressed in mm), and $\sigma_{\mathrm{R}}^2 = 1.23 C_{\mathrm{n}}^2 k^{7/6} L^{11/6}$ represents the Rytov variance, here C_{n}^2 is the refractive index structure parameter used to define the intensity of turbulence, and L is the propagation distance.

$$\sigma_{\mathrm{ls}}^2(L_0) = 0.04\sigma_1^2 \left(\frac{\eta_{\mathrm{Xa_0}} Q_{\mathrm{ls}}}{\eta_{\mathrm{Xa_0}} + Q_{\mathrm{ls}}}\right)^{7/6} \left[1 + 1.75\left(\frac{\eta_{\mathrm{Xa_0}}}{\eta_{\mathrm{Xa_0}} + Q_{\mathrm{ls}}}\right)^{1/2} - 0.25\left(\frac{\eta_{\mathrm{Xa_0}}}{\eta_{\mathrm{Xa_0}} + Q_{\mathrm{ls}}}\right)^{7/12}\right] \tag{12}$$

where:

$$\eta_{\mathrm{Xa_0}} = \frac{\eta_{\mathrm{Xa}} Q}{\eta_{\mathrm{Xa}} + Q} \tag{13}$$

$$Q = \frac{64\pi^2 L}{k L_0^2} \tag{14}$$

and $d = \sqrt{k(2a)^2/4L}$ is the equivalent aperture diameter, where a denotes the receiver aperture radius, while L_0 represents large-scale eddies.

The expression for determining the CDF is given by the equation:

$$F_{\gamma_2}(\gamma_2) = \int_0^{\gamma_2} f_{\gamma_2}(\gamma_2)\,\mathrm{d}\gamma_2 \tag{15}$$

By substituting Eq. (4) into (15) and applying the integral solving rule (07.34.21.0084.01) from Ref. [16], the expression for the CDF is obtained:

$$F_{\gamma_2}(\gamma_2) = \sum_{p=0}^{\infty} \frac{2^{b+p-2}\xi^2 K^p \Gamma(b+\xi^2+1)\exp(-K)}{\pi(b+\xi^2)\Gamma(p+1)p!\Gamma(b)\Gamma(b+\xi^2)} \times G_{4.4}^{3.3}\left(\begin{matrix}1, \frac{1-b}{2}, \frac{2-b}{2}, \frac{2+\xi^2}{2} \\ \frac{\xi^2}{2}, \frac{p+1}{2}, \frac{p+2}{2}, 0\end{matrix}\middle| \frac{4(K+1)^2\xi^4\gamma_2}{(\xi^2+1)^2(b-1)^2\mu_2}\right) \tag{16}$$

2.1. Statistical characteristics of the one-hop hybrid RF/FSO system based on selective combining

In the RF/FSO system, a selective combining scheme is adopted, which is implemented by comparing the SNR of the RF/FSO link with the output signal of the maximum SNR [14]:

$$\gamma = \max(\gamma_1, \gamma_2) \tag{17}$$

where γ_1 and γ_2 are the SNRs of the RF and FSO links, respectively. According to this, assuming statistical independence between the RF and FSO channels, the CDF of the hybrid RF/FSO system under is obtained as the product of the individual CDFs [18]:

$$F_\gamma(\gamma) = P_\mathrm{r}(\max(\gamma_1, \gamma_2) \le \gamma) = P_\mathrm{r}(\gamma_1 \le \gamma, \gamma_2 \le \gamma) = F(\gamma_1)F(\gamma_2) \tag{18}$$

By substituting Eqs. (3) and (16) into Eq. (18) and applying the product rule of Meijer's functions, the generalized extended form of the bivariate Meijer-G function (EGBMGF – extended generalized bivariate Meijer-G function; rule (07.34.16.0003.01) from Ref. [16]) is obtained, which represents the CDF of the hybrid RF/FSO system.

$$F_\gamma(\gamma) = \sum_{p=0}^{\infty} \frac{2^{b+p-2}\xi^2 K^p \Gamma(b+\xi^2+1)\exp(-K)}{\pi(b+\xi^2)\Gamma(m)\Gamma(p+1)p!\Gamma(b)\Gamma(b+\xi^2)} \times G_{0.0,\,1.2,\,4.4}^{0.0,\,1.1,\,3.3}\left(\begin{matrix}1 \\ m, 0\end{matrix}\middle| \begin{matrix}1, \frac{1-b}{2}, \frac{2-b}{2}, \frac{2+\xi^2}{2} \\ \frac{\xi^2}{2}, \frac{p+1}{2}, \frac{p+2}{2}, 0\end{matrix}\middle| m\frac{\gamma_1}{\mu_1}\middle| \frac{4(K+1)^2\xi^4\gamma_2}{(\xi^2+1)^2(b-1)^2\mu_2}\right) \tag{19}$$

2.2. ABER of the one-hop hybrid RF/FSO system

For the hybrid RF/FSO system, the expression for determining the ABER is derived from the following expression:

$$P_{\mathrm{ABER}}(\gamma) = \frac{y^x}{2\Gamma(x)}\int_0^\infty \exp(-y\gamma)\gamma^{x-1}F_\gamma(\gamma)\,\mathrm{d}\gamma \tag{20}$$

where x and y represent the ABER parameters for the binary modulation scheme. Table 1 shows the values of x and y parameters depending on the modulation.

T a b l e 1. Values of x and y parameters depending on the modulation technique.

Modulation technique	x	y
Coherent binary phase shift keying (CBPSK)	0.5	1
Coherent binary frequency shift keying (CBFSK)	0.5	0.5
Non-coherent binary frequency shift keying (NBFSK)	1	0.5
Diferential binary phase shift keying (DBPSK)	1	1

By substituting Eq. (19) into Eq. (20), implementing the CBPSK modulation technique, and applying the rule (01.03.26.0004.01) from Ref. [16], where $\exp(-y\gamma) = G_{01}^{10}(y\gamma|_0^-)$, and then applying the rule (07.34.21.0081.01) from Ref. [16], the expression for the ABER of the hybrid RF/FSO one-hop transmission system is obtained:

$$P_\gamma(\gamma) = \sum_{p=0}^{\infty} \frac{2^{b+p-3}\xi^2 K^p \Gamma(b+\xi^2+1)\exp(-K)}{\pi(b+\xi^2)\Gamma(m)\Gamma(x)\Gamma(p+1)p!\Gamma(b)\Gamma(b+\xi^2)} \times G_{10,\,1.2,\,4.4}^{01,\,1.1,\,3.3}\left(\begin{matrix}0 \\ - \end{matrix}\middle|\begin{matrix}1 \\ m,\,0\end{matrix}\middle|\begin{matrix}1,\,\frac{1-b}{2},\,\frac{2-b}{2},\,\frac{2+\xi^2}{2} \\ \frac{\xi^2}{2},\,\frac{p+1}{2},\,\frac{p+2}{2},\,0\end{matrix}\middle|\frac{m}{\mu_1}\middle|\frac{(K+1)^2\xi^4}{2(\xi^2+1)^2(b-1)^2\mu_2}\right) \tag{21}$$

By substituting Eq. (16) into Eq. (20), applying the CBPSK modulation technique, and solving the integral using the rule (07.34.21.0088.01) from Ref. [16], the expression for the ABER from the source to the receiver node for FSO only is obtained:

$$P_{\gamma_2}(\gamma_2) = \sum_{p=0}^{\infty} \frac{2^{b+p-3}\xi^2 K^p \Gamma(b+\xi^2+1)\exp(-K)}{\pi(b+\xi^2)\Gamma(p+1)p!\Gamma(b)\Gamma(b+\xi^2)\Gamma(x)} \times G_{5.4}^{3.4}\left(\begin{matrix}1-x,\,1,\,\frac{1-b}{2},\,\frac{2-b}{2},\,\frac{2+\xi^2}{2} \\ \frac{\xi^2}{2},\,\frac{p+1}{2},\,\frac{p+2}{2},\,0\end{matrix}\middle|\frac{4(K+1)^2\xi^4}{(\xi^2+1)^2(b-1)^2\mu_2}\right) \tag{22}$$

3. Results and discussion

The performance of the proposed hybrid RF/FSO system and the standalone FSO system was analyzed using the ABER expressions derived in Eqs. (21) and (22). The simulation parameters are listed in Table 2. All results were obtained under the assumption that both links share the same average SNR ($\mu_1 = \mu_2$).

T a b l e 2. Parameter values used for numerical calculations.

Parameter description	Notation	Value
Refractive index – the strength of turbulence	C_n^2 [$m^{-2/3}$]	6×10^{-15} (weak) 2×10^{-14} (moderate) 1.2×10^{-13} (strong)
Wavelength	λ [nm]	1000
Distance between transmitter and receiver	L [m]	1200
Received power at the receiver	Ω	1
Receiver sensitivity	R [A/W]	1
Noise variance	σ_N	10^{-7}
Radius of the circular detector	a [m]	0.05
Radius of the optical beam at distance	w_L [m]	0.5
Large-scale eddies	L_0 [m]	0.8
Small-scale eddies	l_0 [mm]	6

By analyzing the graphs, it can be concluded that the ABER level is significantly lower for the hybrid RF/FSO system compared to the FSO system, indicating that the application of the hybrid model improves system performance. It can also be observed that the ABER value decreases as the electrical SNR value increases. Additionally, ABER can be further reduced by increasing the *K*-factor value, which improves the performance of both the FSO and hybrid systems.

Figure 1 illustrates the ABER performance of the hybrid RF/FSO system under strong turbulence for various values of the Rician *K*-factor. It is evident that increasing the *K*-factor significantly improves performance due to the strengthening of the direct signal component. Figure 2, presenting the FSO-only counterpart, shows noticeably higher ABER under the same conditions, confirming the hybrid system's robustness.

Figures 3 and 4 compare ABER performance under weak, moderate, and strong turbulence. Although the Chi-square–inverse Gamma turbulence model was originally derived under an IM/DD detection assumption, the CDF-based performance behavior shown in Fig. 4 remains representative for coherent detection as well. The ABER analysis in this work, including Figs. 1–3, uses CBPSK-specific parameters in the integration framework (Eq. (20)), which ensures consistency with coherent transmission assumptions. Therefore, Fig. 4 serves to illustrate the impact of turbulence regimes on the FSO channel, regardless of the detection method.

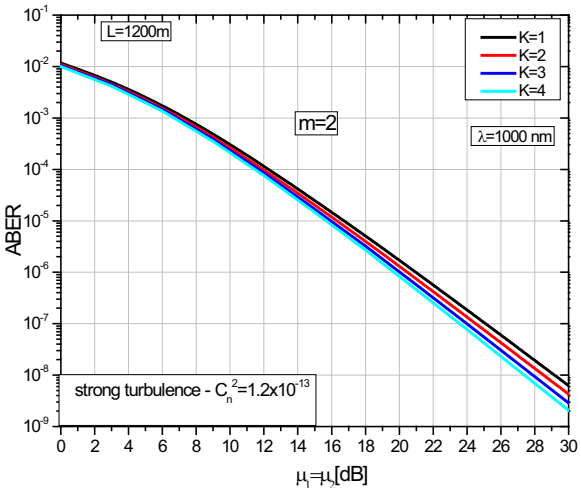

Fig. 1. ABER for the hybrid one-hop RF/FSO system under strong turbulence conditions for different values of the *K*-factor when the CBPSK modulation technique is applied.

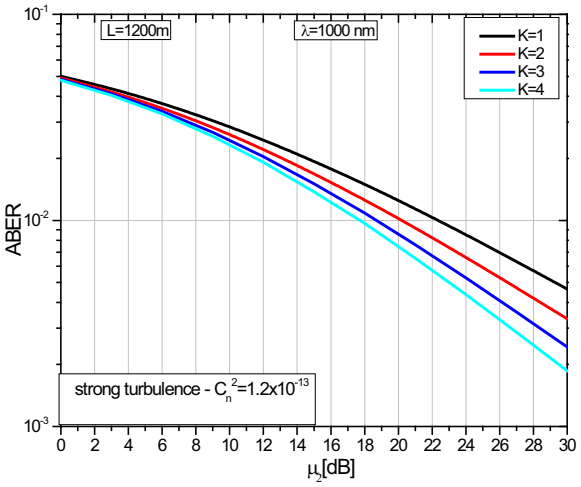

Fig. 2. ABER for the FSO system under strong turbulence conditions for different values of the *K*-factor when the CBPSK modulation technique is applied.

The hybrid system consistently outperforms the FSO link across all regimes. This improvement is attributed to the selective combining scheme, where the RF link compensates for performance degradation in the FSO path. The gap widens with increasing turbulence, highlighting the hybrid system's adaptability to severe atmospheric conditions.

From the graph, it can be observed that for weaker turbulence conditions, the ABER value is lower for both the hybrid and the FSO system. The hybrid RF/FSO system shows slightly higher resistance to atmospheric turbulence compared to the FSO link,

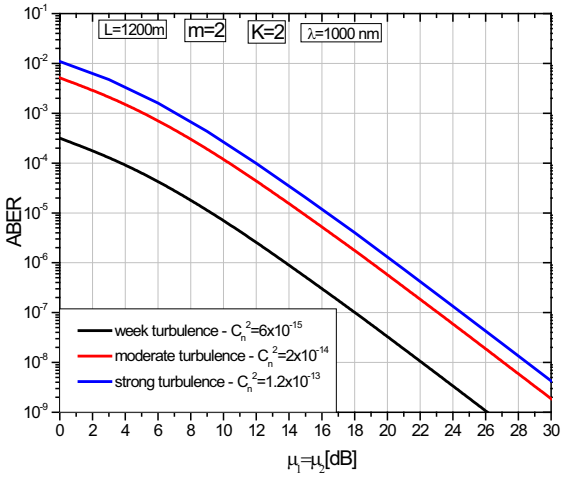

Fig. 3. ABER for the hybrid one-hop RF/FSO system under weak, moderate, and strong turbulence conditions for values $K = 2$ and $m = 2$ when applying the CBPSK modulation technique.

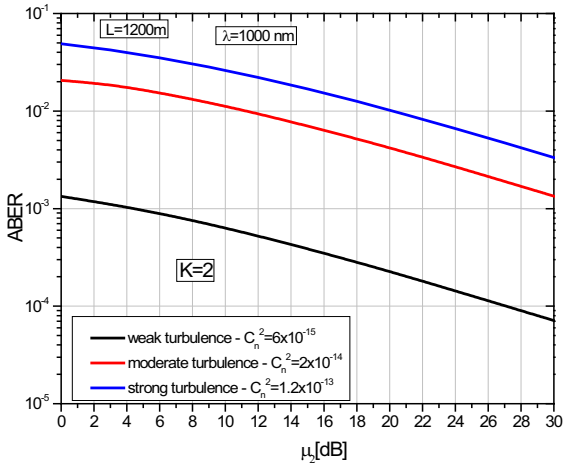

Fig. 4. ABER for the FSO system under weak, moderate, and strong turbulence conditions for $K = 2$ when applying the CBPSK modulation technique.

which was expected. In the hybrid RF/FSO system, when FSO performance degrades due to turbulence effects, the RF link takes over the transmission, and since RF is minimally affected by turbulence, the overall transmission characteristics remain better.

In Fig. 5, the ABER is evaluated as a function of pointing error (quantified via parameter ξ). A smaller ξ implies higher jitter and misalignment, which degrades performance. As ξ increases, both systems benefit, but the hybrid model maintains a consistent advantage, particularly at higher SNR values, where misalignment has a more pronounced effect.

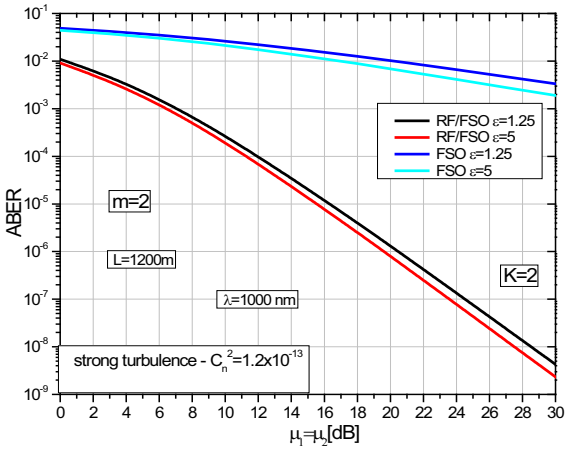

Fig. 5. ABER for the hybrid one-hop RF/FSO and FSO systems as a function of pointing error.

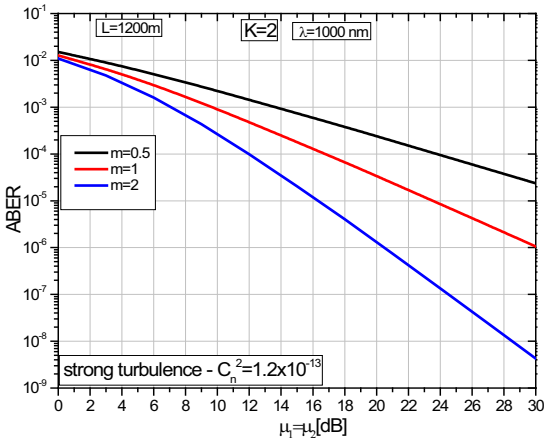

Fig. 6. ABER for the one-hop hybrid RF/FSO system under weak turbulence conditions for different fading statistics values when using the CBPSK modulation technique.

Figure 6 investigates the influence of the Nakagami-*m* fading parameter on the hybrid system under weak turbulence. As expected, increasing mm yields better performance, since higher values correspond to less severe fading. The hybrid system demonstrates considerable sensitivity to mm, particularly in low-to-moderate SNR regimes.

For the initial and lowest value of this parameter, the value $m = 0.5$ was selected, which is also the boundary (lowest) value of this parameter. What can be observed from the graph is that for $m = 0.5$, the ABER level is the highest, and as the value of the parameter m increases, the ABER value decreases, leading to improved system performance. Increasing the electrical SNR further reduces the ABER values, thereby enhancing the system's performance.

Overall, the results validate that the proposed hybrid RF/FSO model exhibits superior performance across diverse turbulence strengths, pointing error levels, and fading conditions. Its resilience stems from the complementary characteristics of RF and optical links, and the effectiveness of selective combining in mitigating link impairments.

4. Conclusion

In order to enhance FSO communication systems, this paper presented a new hybrid RF/FSO model for performance analysis, which combines two independent statistical models. In this process, new expressions for ABER were introduced, determining the performance of the hybrid RF/FSO system and the performance of the FSO system with direct line-of-sight signal propagation when applying CBPSK modulation. A comparative analysis of the performance of these two systems was conducted for different system parameter values, misalignment errors, and levels of atmospheric turbulence.

Thanks to the analysis and research, several very important conclusions have been established. Proposed hybrid one-hop RF/FSO system significantly outperforms the FSO-only system under all evaluated scenarios. Notably, the hybrid scheme exhibits strong resilience to atmospheric turbulence and pointing errors, maintaining reliable transmission by adaptively switching between RF and FSO links based on instantaneous SNR conditions. This dynamic switching mechanism ensures continuous data flow and minimal outage probability, making the system particularly effective in urban environments, high-altitude platforms, and emergency communication.

It can also be concluded that the *K*-factor has a significant impact on improving the performance of both the FSO and hybrid RF/FSO systems. Additionally, the hybrid RF/FSO system is characterized by the *m* parameter, the increase of which can have a major impact on improving the performance of the hybrid RF/FSO system. These findings validate the effectiveness of the proposed statistical model and highlight the practical viability of hybrid RF/FSO links in real-world deployments.

References

[1] Nadeem F., Kvicera V., Awan M.S., Leitgeb E., Muhammad S.S., Kandus G., *Weather effects on hybrid FSO/RF communication link*, IEEE Journal on Selected Areas in Communications **27**(9), 2009: 1687-1697. https://doi.org/10.1109/JSAC.2009.091218

[2] Wu H., Kavehrad M., *Availability evaluation of ground-to-air hybrid FSO/RF links*, International Journal of Wireless Information Networks **14**(1), 2007: 33-45. https://doi.org/10.1007/s10776-006-0042-1

[3] Nadeem F., Leitgeb E., Awan M.S., Kandus G., *FSO/RF hybrid network availability analysis under different weather condition*, [In] *2009 Third International Conference on Next Generation Mobile Applications, Services and Technologies*, Cardiff, UK, 2009: 239-244. https://doi.org/10.1109/NGMAST.2009.34

[4] Kong L., Xu W., Hanzo L., Zhang H., Zhao C., *Performance of a free-space-optical relay-assisted hybrid RF/FSO system in generalized M-distributed channels*, IEEE Photonics Journal **7**(5), 2015: 7903319. https://doi.org/10.1109/JPHOT.2015.2470106

[5] NAJAFI M., JAMALI V., SCHOBER R., *Optimal relay selection for the parallel hybrid RF/FSO relay channel: Non-buffer-aided and buffer-aided designs*, IEEE Transactions on Communications **65**(7), 2017: 2794-2810. https://doi.org/10.1109/TCOMM.2017.2686868

[6] UPADHYA A., MEENALAKSHMI M., CHATURVEDI S., DWIVEDI V.K., *Full duplex mixed FSO/RF relaying systems with self-interference and outdated CSI*, Optical and Quantum Electronics **55**, 2023: 3. https://doi.org/10.1007/s11082-022-04265-8

[7] MOULSLEY T., VILAR E., *Experimental and theoretical statistics of microwave amplitude scintillations on satellite down-links*, IEEE Transactions on Antennas and Propagation **30**(6), 1982: 1099-1106. https://doi.org/10.1109/TAP.1982.1142964

[8] HE B., SCHOBER R., *Bit-interleaved coded modulation for hybrid RF/FSO systems*, IEEE Transactions on Communications **57**(12), 2009: 3753-3763. https://doi.org/10.1109/TCOMM.2009.12.080396

[9] WU H., HAMZEH B., KAVEHRAD M., *Achieving carrier class availability of FSO link via a complementary RF link*, [In] *Conference Record of the Thirty-Eighth Asilomar Conference on Signals, Systems and Computers, 2004*, Vol. 2, Pacific Grove, CA, USA, 2004: 1483-1487. https://doi.org/10.1109/ACSSC.2004.1399401

[10] JIA Z., AO F., ZHU Q., *BER performance of the hybrid FSO/RF attenuation system*, [In] *2006 7th International Symposium on Antennas, Propagation & EM Theory*, Guilin, China, 2006: 1-4. https://doi.org/10.1109/ISAPE.2006.353532

[11] SIMON M.K., ALOUINI M.-S., *Digital Communication Over Fading Channels*, Wiley-Interscience, NJ, USA, 2nd Ed., 2005. https://doi.org/10.1002/0471715220

[12] USMAN M., YANG H.-C., ALOUINI M.-S., *Performance analysis of switching based hybrid FSO/RF transmission*, [In] *2014 IEEE 80th Vehicular Technology Conference (VTC2014-Fall)*, Vancouver, BC, Canada, 2014: 1-5. https://doi.org/10.1109/VTCFall.2014.6966119

[13] USMAN M., YANG H.-C., ALOUINI M.-S., *Practical switching-based hybrid FSO/RF transmission and its performance analysis*, IEEE Photonics Journal **6**(5), 2014: 7902713. https://doi.org/10.1109/JPHOT.2014.2352629

[14] SHAKIR W.M.R., *On performance analysis of hybrid FSO/RF systems*, IET Communications **13**(11), 2019: 1677-1684. https://doi.org/10.1049/iet-com.2018.5147

[15] VISHWAKARMA N., SWAMINATHAN R., *Performance analysis of hybrid FSO/RF communication over generalized fading models*, Optics Communications **487**, 2021: 126796. https://doi.org/10.1016/j.optcom.2021.126796

[16] https://mathworld.wolfram.com

[17] STANOJEVIĆ N., BANĐUR Đ., MOSUROVIĆ L., SPALEVIĆ P., PANIĆ S., *Exploring a novel turbulence model: The Chi-square/inverse Gamma approach for enhanced free space optics (FSO) communication*, Optica Applicata **54**(3), 2024: 337-351. https://doi.org/10.37190/oa240305

[18] AMIRABADI M.A., VAKILI V.T., *Performance comparison of two novel relay-assisted hybrid FSO/RF communication systems*, IET Communications **13**(11), 2019: 1551-1556. https://doi.org/10.1049/iet-com.2018.5469

Received June 11, 2025
in revised form August 6, 2025